Cardiovascular Engineering and Technology, Vol. 10, No. 1, March 2019 *(© 2019)* pp. 10–21
https://doi.org/10.1007/s13239-019-00401-w

Multi-Objective Optimization Design of Balloon-Expandable Coronary Stent

XIANG SHEN, HONGFEI ZHU, JIABAO JIANG, YONGQUAN DENG, and SONG JI

Department of Mechanical Engineering, Jiangsu University, No. 301, Xuefu Road, Zhenjiang, China

(Received 21 August 2018; accepted 11 January 2019; published online 23 January 2019)

Associate Editor Dr. Ajit P. Yoganathan and Dr. James E. Moore oversaw the review of this article.

Abstract
Purpose—Recent studies suggested that suboptimal delivery and longitudinal stent deformation can result in in-stent restenosis. Therefore, the purpose of this paper was to study the effect of stent geometry on stent flexibility and longitudinal stiffness (LS) and optimize the two metrics simultaneously. Then, the reliable and accurate relationships between metrics and design variables were established.
Methods—A multi-objective optimization method based on finite element analysis was proposed for the investigation and improvement of stent flexibility and LS. The relative influences of design variables on the two metrics were evaluated on the basis of the main effects. Three surrogate models, namely, the response surface model (RSM), radial basis function neural network (RBF), and Kriging were employed and compared.
Results—The accuracies of the three models in fitting flexibility were nearly similar, although Kriging made more accurate prediction in LS. The link width played important roles in flexibility and LS. Although the flexibility of the optimal stent decreased by 13%, the LS increased by 48.3%.
Conclusions—The obtained results showed that the multi-objective optimization method is efficient in predicting an optimal stent design. The method presented in this paper can be useful in optimizing stent design and improving the comprehensive mechanical properties of stents.

Keywords—Coronary stents, Multi-objective optimization, Flexibility, Longitudinal stiffness.

INTRODUCTION

Vascular stents are tubular supports that open narrow lesions and remodel blood flow environments.[5,12,20] Although more efficient than traditional surgery, stenting may cause in-stent restenosis (ISR) and stent thrombosis (ST).[27,39] The causes of ISR and ST have not been completely understood, although some contributing factors have been identified. For example, considered a major cause of ISR,[4,11,13] stents with insufficient flexibility may cause tissue damage after implantation. Stents with small longitudinal stiffness (LS) are prone to longitudinal deformation, which results in stent malapposition and inflammation and promotes ST formation.[16,32]

Previous studies suggested that flexibility and LS have considerable effects on the long-term outcomes of balloon-expandable stents.[4,32] Flexibility has been considered an extremely important goal in stent design,[6] and finite element analysis (FEA) has been preferred in stent numerical studies.[10,22–25] For example, Ju *et al.*[15] adopted FEA to study flexibility in stents with different link configurations and found that stents without links are less flexible. Perini *et al.*[30] used the experimental method to study the connection between flexibility and link shape. Their results showed that stents with links have more crests and are more flexible than stents without links. Recently, LS has been confirmed as a key parameter because low LS correlates with increased incidence of longitudinal stent deformation.[8,37] Ormiston *et al.*[26] after compressing seven modern clinical stents, found that LS decreases with link number. Shen *et al.*[34] used FEA to analyze longitudinal deformation in stents by using different parameters. Their results indicated that longitudinal deformation can be effectively reduced by optimizing the design parameters of stents.

Moreover, stent flexibility and LS conflict with each other[6,16] That is, improving the performance of one can decrease the performance of another. For example, increasing the number of links or altering the geometries of the links enhances stent LS but may reduce stent flexibility.[26] Most of the above-mentioned studies examined the two factors separately and neglected the

Address correspondence to Xiang Shen, Department of Mechanical Engineering, Jiangsu University, No. 301, Xuefu Road, Zhenjiang, China. Electronic mail: sx@ujs.edu.cn

trade-off between them. Moreover, a comprehensive study of flexibility and LS was lacking, and the potential relationships between them remains unknown. The multi-objective optimization method has been proven efficient in solving such problems[2] and thus has been extensively used in stent optimization, although different surrogate models were adopted by different researchers. For example, Azaouzi *et al.*[1] constructed response surface models (RSM) and studied the effects of stent thickness, length, and width on stent volume, radial force, and strain amplitude. Shen *et al.*[35] constructed radial basis function (RBF) neural network models and studied the relationships of stent design parameters with collapse and expansion pressure. Ragkousis *et al.*[31] combined FEA and Kriging surrogate models to predict the optimal stent dilation for a given patient-specific model. The purpose of this paper was to study the effect of stent geometry on stent LS and flexibility and compare surrogate models. FEA was adopted to simulate stent axial compression after expansion and stent bending, and RSM, RBF, and Kriging were constructed for each metric. The surrogate model with the best accuracy was selected to search the Pareto front with a non-dominated sorting genetic algorithm (NSGA-II).

MATERIALS AND METHODS

Stent Geometry

The generic balloon-expandable stent used in our study[34] is shown in Fig. 1. It was composed of a strut and a link part (Fig. 1a). The strut part is a crown-shaped ring and composed of eight repeating waved units (Fig. 1b) in the circumferential direction. Stent link shape varies (I, S, U, or V shape). We preferred stents with S-shaped links because they have the lowest propensity to cause restenosis.[29] These stents are individually composed of six struts and five rows of links and distribute uniformly in the circumferential direction to connect adjacent struts, as shown in Fig. 1. Strut width (W_{struct}), which dictates stent LS[9] and link width (W_{link}), which greatly influences stent flexibility[33] were selected as optimization variables in our study. Meanwhile, Ormiston *et al.*[26] found that stent thickness (T) is a major contributor to stent flexibility and LS. For example, a thin stent shows improved flexibility but reduced stent LS. Their study confirmed that stent flexibility and LS conflict with one another. Therefore, we also considered T as one of the design variables. Figure 2 shows the definitions of the variables.

The stent used in our study was modeled with Pro/Engineer 5.0 (Parametric Technology Corp., Waltham, MA, USA) and had an inner diameter of 1.79 mm and length of 9 mm. The variables are listed in Table 1.

Material

The balloon-expandable stent material was medical 316L stainless steel, which is the most widely used material for bare metal stents. The 316L stainless steel mechanical behavior was modeled by using a homogeneous, isotropic, and elastoplastic material with nonlinear hardening behavior. We used the following parameters to demonstrate the material: Young's modulus, 201 GPa; yield stress, 330 MPa; Poisson's ratio, 0.3; limit stress, 750 MPa; and density, 7.86 g/cm^3.[34]

Simulation

The ABAQUS/Standard (Dassault Systems Simulia Corp., Rhode Island, USA) finite element solver was adopted to carry out the computational simulations.

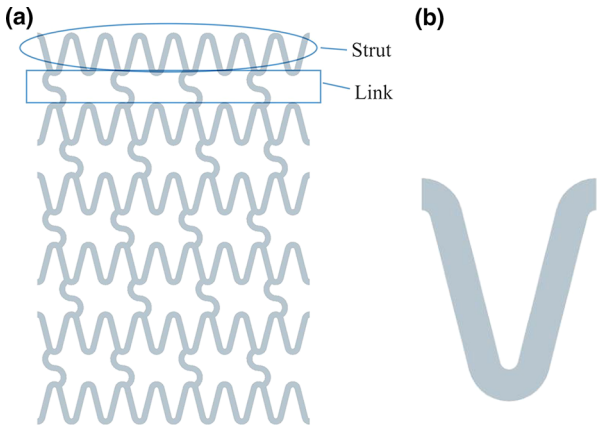

FIGURE 1. Two-dimensional sketches of the balloon-expandable stent.

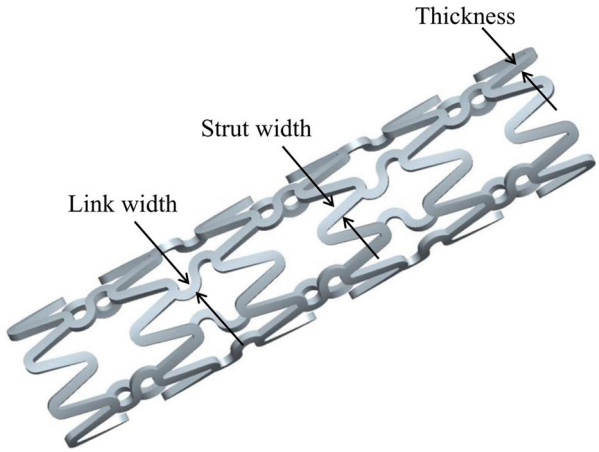

FIGURE 2. Stent geometric parameters definition.

Flexibility

The response of a part of a stent differs from that of a full-length stent in flexibility analysis.[30] Therefore, a whole stent model was adopted to simulate stent flexibility. An eight-node linear brick solid element (C3D8R) was used to mesh the stent. To evaluate stent flexibility, we used the four-point bending method proposed by Wu *et al.*[38]

As shown in Fig. 3, two reference points were established at the intersection of the left and right ends of the stent and central axis. Then, the nodes at each end were coupled to their respective reference points. Reference point 1 (RP-1) was fixed on the x, y, and z directions, and reference point 2 (RP-2) was fixed on the x and y directions. The rotation around the z direction was constrained on RP-1 and RP-2. A self-contact algorithm was applied in the simulation to prevent the self-penetration of the stent.[4] Bending deformation was then applied at each reference point, and 30° was the corresponding angle.

Longitudinal Stent Compression

As shown in Fig. 4, longitudinal stent compression FEA model included a stent and two rigid flats, which were parallel to the end surfaces of the stent and had overlapping middle points. The flats were meshed with four-node bilinear rigid quadrilateral element (R3D4). Two reference points were set up at the center of each flat for the calculation of stent LS. Surface-to-surface contact with a 0.2 frictional coefficient[29] was applied between the ends of the stent and the two flats. The complete longitudinal stent compression simulation included the following three steps:

TABLE 1. Abbreviations and ranges of variables.

Variables	Abbreviations	Lower bound (mm)	Upper bound (mm)
Thickness	T	0.06	0.14
Link width	W_{link}	0.06	0.14
Strut width	W_{struct}	0.08	0.16

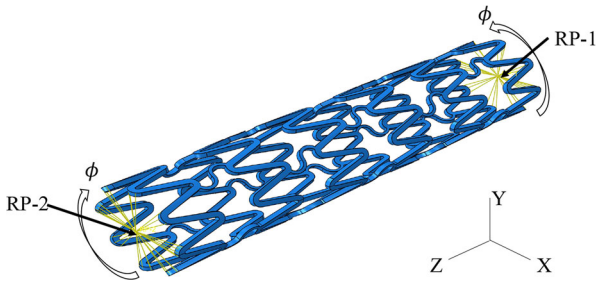

FIGURE 3. Constraints applied in the flexibility analysis.

Step 1 Stent inner diameter was expanded to 3.0 mm;
Step 2 Stent recoiled;
Step 3 the right flat compressed the stent

In the first step, the nodes of the stent left end were fixed in the axial direction, and the rotation of all nodes on the left and right ends were constrained in the circumferential direction. Thus, stent rigid-body movement did not occur. Then, we applied 0.6 mm radial displacement on the inner wall of the stent to cause a balloon-like expansion. In the second step, the boundary conditions were maintained, but the radial displacement was removed and the stent recoiled after expansion. In the third step, the left flat was fixed, and we moved the right flat 1.5 mm to the left to simulate the stent longitudinal deformation caused by other devices, such as guide catheters or imaging tools.

Objective Functions

Flexibility Metric

The flexibility of the stent can be measured by the area of moment–curvature curve.[27] The flexibility metric (FM), can be calculated as follows:

$$\text{FM} = \int_0^{\chi_{\max}} M(\chi)\mathrm{d}\chi \tag{1}$$

where M was the bending moment and χ was the corresponding curvature. Equation (2) shows the definition of χ.

$$\chi = 2\phi / L_{\text{stent}} \tag{2}$$

where ϕ is the bending angle (Fig. 5), and L_{stent} is the length of the stent. Our present study is different from that of Pant *et al.*[27] In particular, our study adopted a whole stent model to simulate stent flexibility, whereas Pant *et al.*[27] investigated only one unit of a stent.

Longitudinal Stiffness (LS)

LS can be used to quantify the longitudinal compression integrity of a stent.[17] Maleckis *et al.*[17] pointed out that stent LS can be obtained by calculating the slope of the first 20% of the force–displacement curve.

$$U = L_{\text{recoiled}} - L_{\text{compressed}} \tag{3}$$

As given in Eq. (3), U is the axial deformation, L_{recoiled} is the axial length of a stent after recoiling, and $L_{\text{compressed}}$ is the axial length of the stent after longitudinal compression. The LS of the stent was defined as follows:

$$\text{LS} = F/U \tag{4}$$

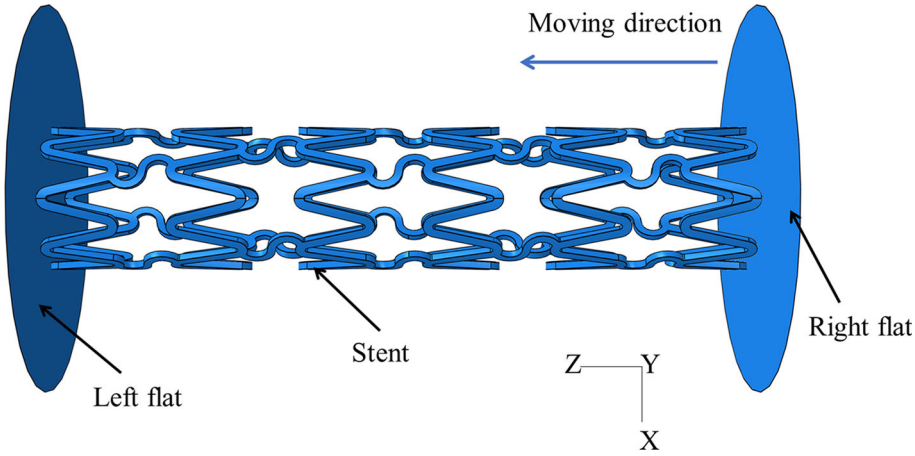

FIGURE 4. Finite element analysis model of stent longitudinal compression.

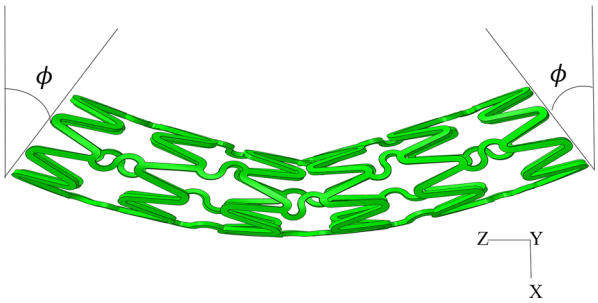

FIGURE 5. Bending angle ϕ applied in the flexibility analysis.

where F is the corresponding force.

Optimization Problem

The commercial software ISIGHT (Dassault Systems Simulia Corp., Rhode Island, USA) was adopted to solve the multi-objective optimization problem.

After defining the above objective functions, the optimization problem in this paper was described as follows:

$$\begin{cases} \text{Minimise FM}(T, W_{\text{struct}}, W_{\text{link}}) \\ \text{Minimise LS}^{-1}(T, W_{\text{struct}}, W_{\text{link}}) \end{cases} \quad (5)$$

Equation (6) depicts the bounds of the variables.

$$\begin{cases} 0.06 \le T \le 0.14 \\ 0.08 \le W_{\text{struct}} \le 0.16 \\ 0.06 \le W_{\text{link}} \le 0.14 \end{cases} \quad (6)$$

LS index should be maximized. However, a reciprocal of the longitudinal stiffness (LS^{-1}) was used in Eq. (5). The purpose of our optimization was to minimize LS^{-1} in order to improve LS. The solution methodology adopted in this study is depicted in Fig. 6. Our work began with the definition of the stent variables. Then, 23 sampling points were obtained by optimal latin hypercube sampling (OLHS).[19] Stent flexibility and longitudinal compression were simulated by FEA. RSM,[21] RBF,[36] and Kriging[18] were constructed on the basis of the obtained objective functions. The errors of the three methods were compared. NSGA-II[3] was used in determining the Pareto optimal solution in the design space.

Sampling Plan

A total of 23 test cases were initially performed with OLHS. The three parameters (T, W_{struct}, and W_{link}) varied among these cases. In contrast to latin hypercube sampling (LHS), OLHS improves the uniformity of the spatial distribution of test points. In some of the cases, some regions of their design spaces were lost with the increases in parameter values. The fitting of factors and responses were accurate. All the 23 initial test cases were subjected to the same boundary conditions, but the three models were excluded from the test samples owing to some convergence problems encountered in FEA analysis. Thus, a total of 20 sample points were ultimately used for the construction of surrogate models.

Surrogate Models

The relationships between objective functions and design variables in stent optimization were complex and implicit. Consequently, surrogate models were constructed to fit the responses. Such methods have been proven efficient in previous vascular stent optimization studies.[7,28,35] However, the studies used different surrogate models. The most commonly used surrogate models were RSM, RBF, and Kriging. We compared the errors of the three models to determine

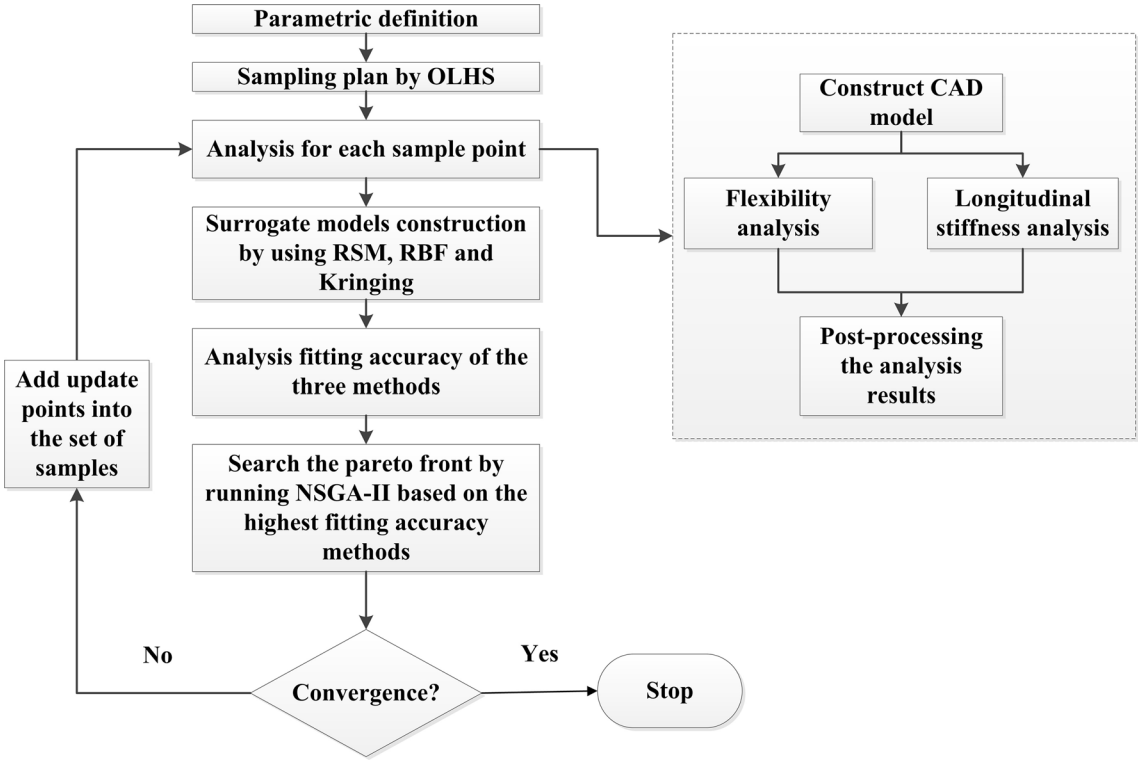

FIGURE 6. Flow chart of the adopted optimization methodology.

the most accurate model in combination with NSGA-II.

NSGA-II

NSGA-II is widely used in the multi-objective optimization of stents[7,28,31] because it has good exploration capabilities. We selected the Gaussian model because it includes the assessment of model non-determinacy, which is represented by the mean square error (MSE).[31] After the surrogate models were constructed, we ran the NSGA-II to determine the trade-off between flexibility and LS. The population size of NSGA-II was 40, the number of generations was 40, and the crossover probability was 0.9.

RESULTS AND DISCUSSIONS

This section first introduced the FEA results for the baseline stent, then the comparison among the surrogate models, and finally the multi-objective optimization study.

Baseline Geometry Results

Results of Stent Flexibility

The results of flexibility simulation are shown in Fig. 7. The link had a large deformation and led to stress concentration. Therefore, the flexibility of the stent was mainly affected by the link, and this finding is consistent with the conclusions of previous experimental and simulation studies.[9,30] After the stent was bent, one side of the link was compressed, and the other side was stretched, as shown in Fig. 7. After the stent bent to an angle, self-contact, which increases resistance to bending, occurred on the compressed side of the stent. Figure 8 shows the relationship between the moment and the curvature index, the M-χ curve. Obviously, the curve can be divided into three parts, as follows:

Part 1	The initial linear part, in which the stent underwent elastic deformation
Part 2	The relatively flat plateau part, which represented the plastic deformation area
Part 3	The self-contact part, where incremental moment can be observed

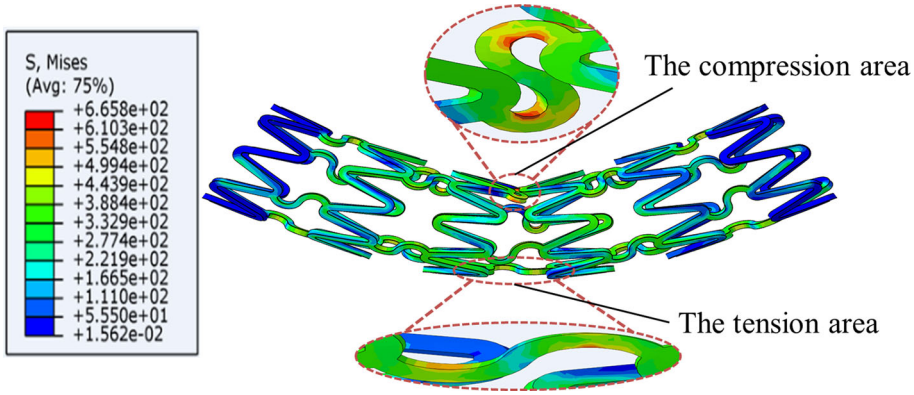

FIGURE 7. Flexibility analysis results for the baseline stent.

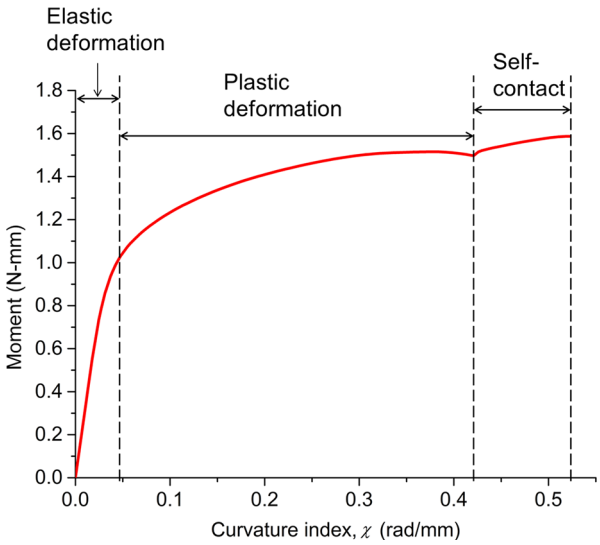

FIGURE 8. Moment–curvature index plot for baseline stent.

The area under the M-χ can be calculated by Eq. (1). The smaller the area is, the better the flexibility of the stent is.

Results of Stent Longitudinal Stiffness

The results of longitudinal stent compression analysis with an axial displacement of 1.5 mm are shown in Fig. 9. The links along with the struts showed remarkable deformation after longitudinal compression, as shown in the graph. This result was different from the flexibility results, which showed that only the links underwent large deformation. Although only axial displacement was applied on the stent, a combined load of compression and torsion was imposed on the stent, as pointed out by Hasio *et al.*[29] The plot between the force and displacement is shown in Fig. 10. The force–displacement curve can be characterized by first a linear part (the elastic deformation part), followed by a stable curved part (the plastic deformation part). The stent LS can be calculated by Eq. (4). The higher the LS is, the better the stent LS is.

Comparison of Different Surrogate Models

On the basis of the initial 20 samples (listed in Table 2), RSM, RBF, and Kriging models for each objective were constructed. The accuracy of the three models[14] was assessed with the leave-one-out principle, in which only one of the original samples was used as verification data. The rest was used as training data. All the samples were validated. Figure 11 shows the leave-one-out plot. The abscissa in the figure was the actual value, and the ordinate was the predicted value. The closeness of the points to the 45 degree line suggested the high accuracy of the model. Figures 12 and 13 show the error analysis results. Equations (7), (8), and (9) provide the modeling error (δ_i), the root mean square error (RMS), and the coefficient of determination (R^2), respectively.

$$\delta_i = |\hat{y}_i - y_i| \; i = 1, 2, \ldots, n_e \tag{7}$$

$$\text{RMS} = \sqrt{\frac{\sum_{i=1}^{n_e} \delta_i^2}{n_e}} \tag{8}$$

$$R^2 = 1 - \left(\frac{\sum_{i=1}^{n_e} (y_i - \hat{y}_i)}{\sum_{i=1}^{n_e} (y_i - \bar{y}_i)} \right) \tag{9}$$

where n_e is the number of the error analysis point, y_i is the value obtained at the ith point from FEA, $\hat{y}$ is the mean value of y_i, and $\hat{y}$ is the predicted value at the ith point. An R^2 of > 0.9 was obtained, and thus the surrogate models predicted the objectives reliably.

As shown in Fig. 12, the R^2 values were all greater than 0.9 in the predictions of FM, indicating good

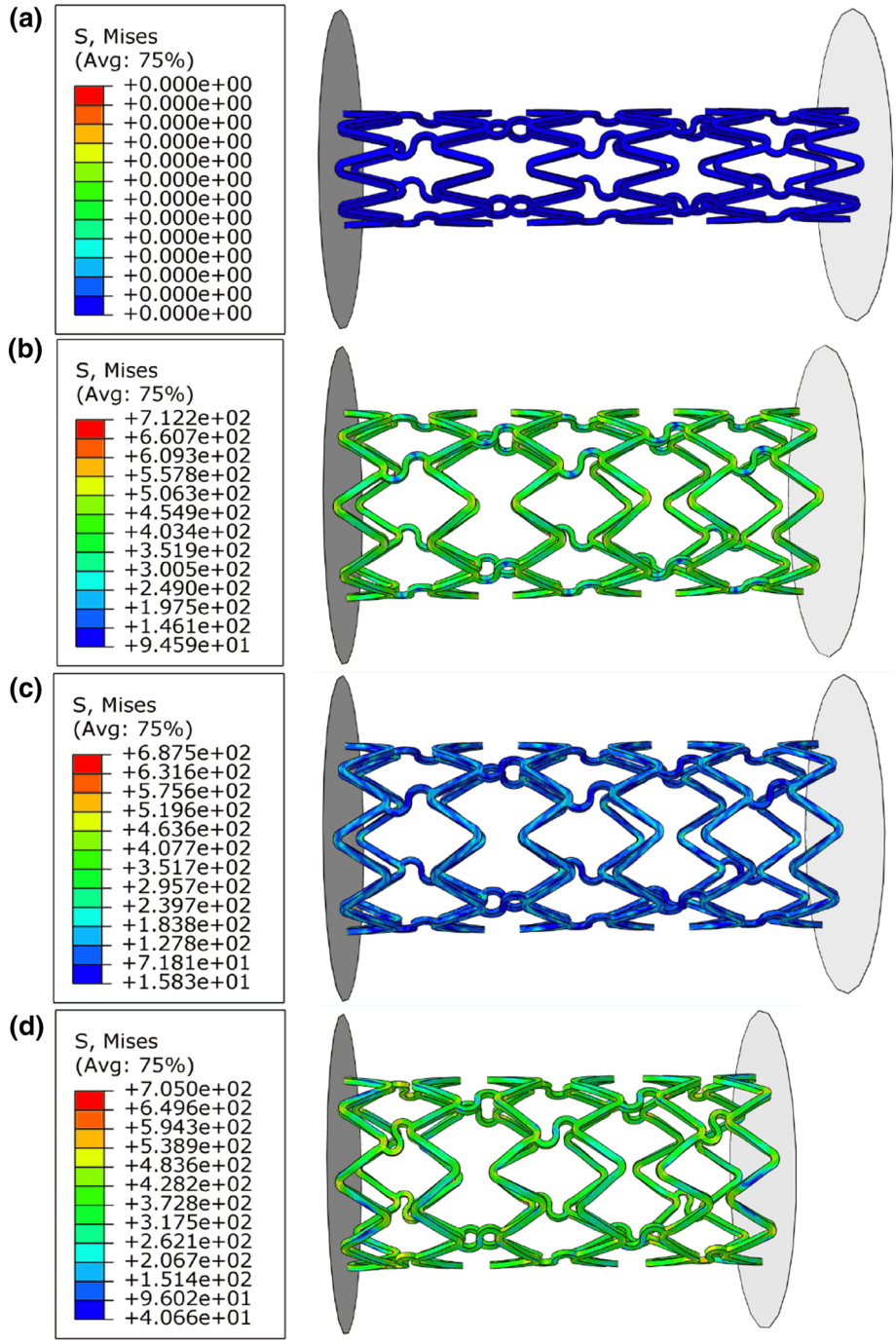

FIGURE 9. Stent longitudinal compression analysis for the baseline geometry: (a) initial shape; (b) expanded shape; (c) recoiled shape; (d) compressed shape.

predictions. Fairly small differences (about 1.48%) were found among the R^2 values, showing that the accuracies of the three models in fitting FM were nearly the same. This is evidently shown in the left column of Fig. 11, where the points in all the models were close to the straight 45° line. Meanwhile, only the R^2 value of Kriging was above 0.9 in the prediction of LS. The R^2 values of the other models were less than 0.9 and thus unreliable.

In Fig. 13, the differences among the RMS values of the three models were large. The RMS values of Kriging, RSM, and RBF were 0.0882, 0.1245 (about 41.16% greater than Kriging), and 0.1201 (about 36.17% greater than Kriging), respectively. Kriging

made the best prediction. It also can be interpreted by the right column of Fig. 11. The points in RSM-LS^{-1} and RBF-LS^{-1} were relatively away from the straight 45° line, and this result demonstrated the large difference between the predicted and actual values. The flexibility simulation encountered deformation only once, whereas the LS simulation underwent deformation two times. Therefore, the relationship between the design variables and LS was more complex than the relationship between the design variables and flexibility. The RSM that encountered deformation only once was slightly accurate in approximating response. When the performance simulation encountered deformations at least two times, Kriging was superior to RBF or RSM.

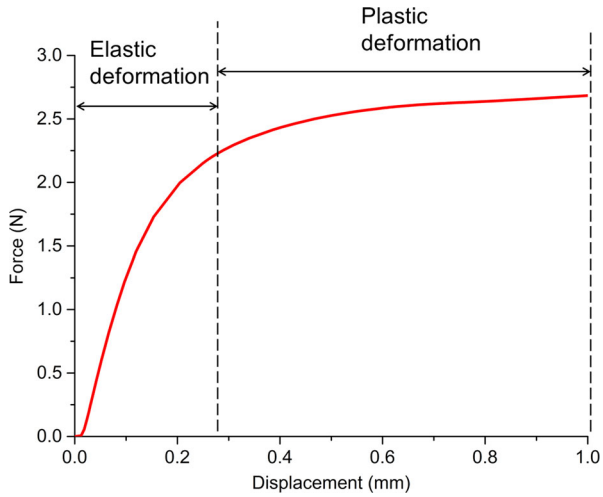

FIGURE 10. Force–displacement plot for baseline stent.

Main Effects

The purpose of this study was to minimize the FM and LS^{-1} simultaneously. The objective functions values of the 20 samples were obtained from the FEA simulations. Figure 14 shows the two metrics. Increased flexibility generally implied decreased LS^{-1}. For the assessment of the effect of each parameter on each objective, the main effects for each response based on the Kriging model are shown in Fig. 15.

The trade-off between flexibility and LS^{-1} can be explained by the main effects. W_{link} considerably affected flexibility and LS, and this finding is consistent with the conclusions obtained by previous studies.[9,34] The high W_{link} implied that the link had additional materials and the force and moment required to compress and bend the stent, respectively, increased. Intuitively, a wide link implied improved stiffness and reduced flexibility.

Optimization Results

Kriging was selected for the next optimization owing to its high accuracy. After the Kriging models were constructed, NSGA-II was adopted to find the optimal solution. A comparison of the optimal stent and baseline stent is shown in Table 3. The optimal stent had a higher link width and strut width than the original stent but a lower thickness. Although link

TABLE 2. Initial training sampling points and respective objective function values.

Samples	W_{link} (mm)	W_{struct} (mm)	T (mm)	FM (N-rad)	LS^{-1} (mm/N)
1	0.1	0.0982	0.1291	0.867	0.1849
2	0.06	0.1127	0.1	0.2685	0.3788
3	0.1182	0.1164	0.0927	0.7800	0.1403
4	0.0891	0.16	0.1255	0.712	0.1398
5	0.1109	0.1418	0.0709	0.5315	0.1917
6	0.0745	0.12	0.1327	0.5742	0.1861
7	0.0855	0.1564	0.0891	0.4437	0.2231
8	0.1291	0.1055	0.14	1.3451	0.0798
9	0.1218	0.08	0.0818	0.441	0.2477
10	0.0964	0.0945	0.0964	0.5773	0.2014
11	0.1255	0.0836	0.1109	0.8838	0.1213
12	0.1036	0.1018	0.0636	0.34695	0.284
13	0.0673	0.0873	0.1218	0.4194	0.2583
14	0.0818	0.1236	0.0782	0.3695	0.2971
15	0.1327	0.1309	0.1182	1.3757	0.0835
16	0.1073	0.1309	0.1364	1.1457	0.0971
17	0.0636	0.1455	0.1109	0.26325	0.3276
18	0.0709	0.0909	0.0745	0.2538	0.4156
19	0.14	0.1382	0.0855	0.9009	0.1103
20	0.0927	0.1273	0.1073	0.6737	0.1611

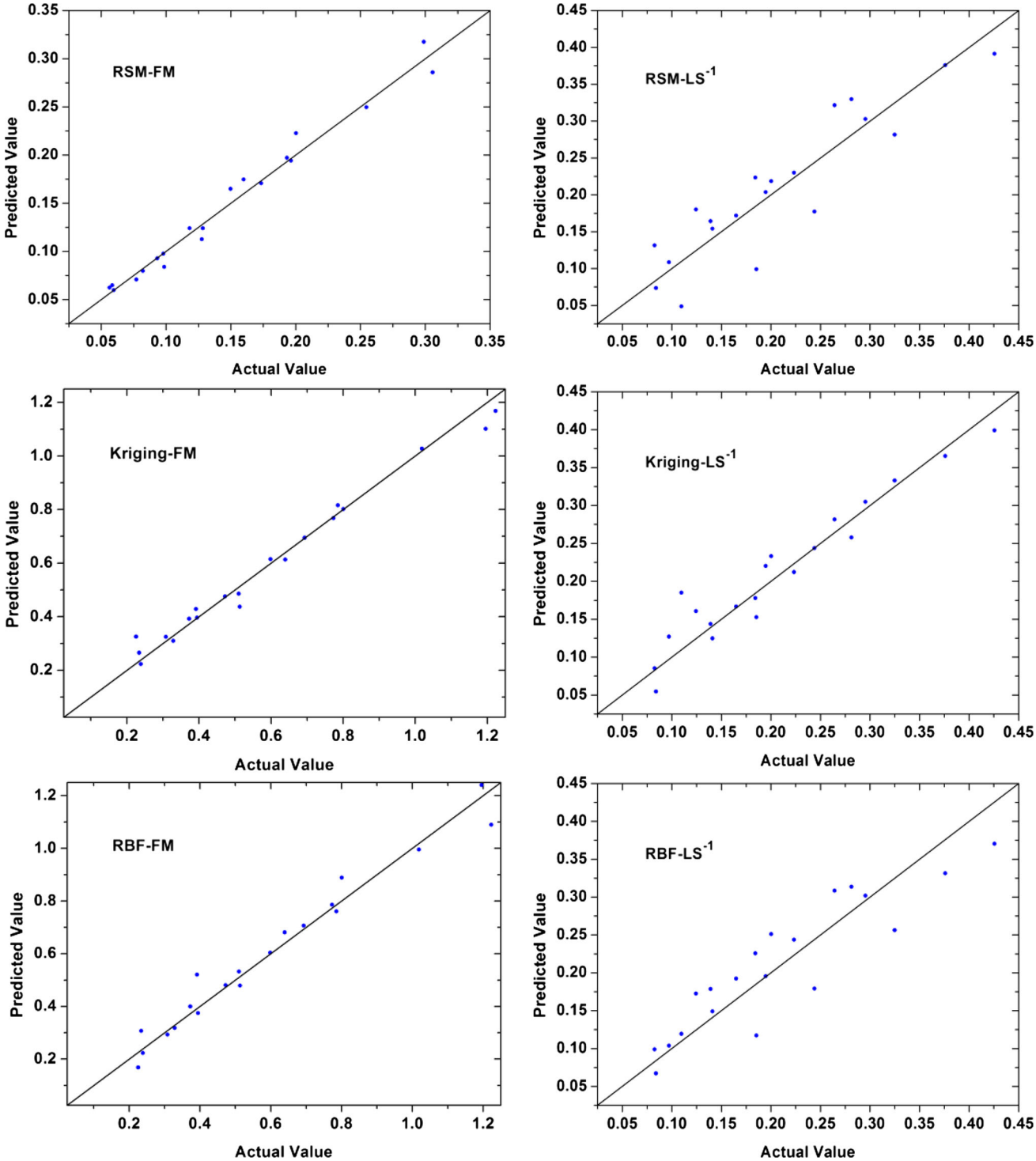

FIGURE 11. RSM, Kriging and RBF models validation: on the left panel, leave-one-point plots for flexibility (FM); on the right panel, leave-one-point plots for longitudinal stiffness (LS^{-1}).

width had the highest influenced on the stent LS, its value only increased by 8.4% in the optimized stent. A high link width reduced the flexibility of the stent possibly because the large stent link width increased the space occupied by the link. Therefore, the possibility of self-contact was high. This phenomenon decreased stent flexibility. The FM value of the optimized stent was 0.7739 N-rad (the predicted value was 0.8016 N-rad, and the error was about 3.6%) and was increased by 13% relative to FM (0.71 N-rad of the

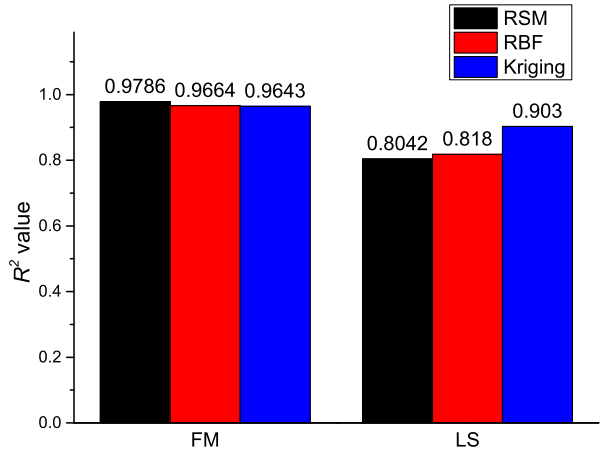

FIGURE 12. R^2 value of RSM, RBF and Kriging surrogate models.

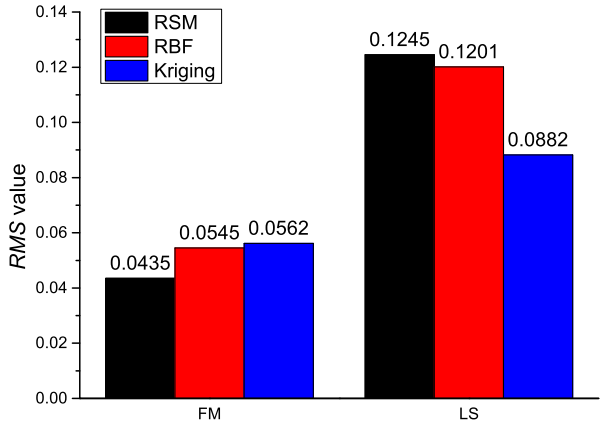

FIGURE 13. *RMS* value of RSM, RBF and Kriging surrogate models.

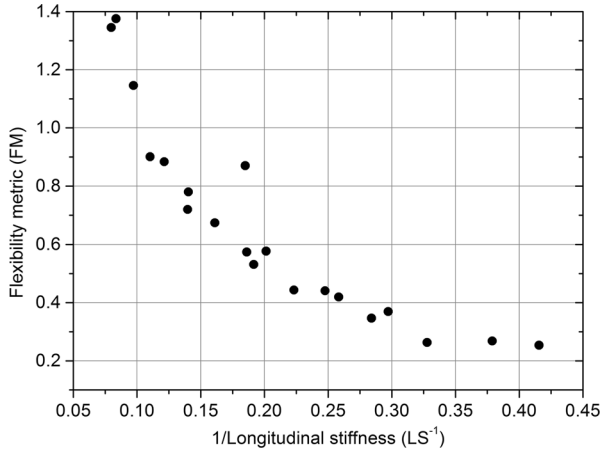

FIGURE 14. Trade-off curve for FM and LS^{-1}.

baseline stent). The LS^{-1} value of the optimized stent was 0.0897 mm/N (the predicted value was 0.0831 mm/N, and the error was about 7.9%) and was 48.3% lower than the LS^{-1} (0.1608 mm/N of the baseline stent). When flexibility and LS were considered, the optimized stent showed improved comprehensive performance.

Study Limitations

The limitations of this paper were as follows: first, the model limitations. Whether in the longitudinal deformation or the flexibility simulation of the stent, the effects of balloon, plaque, and vessel on the stent were not considered. In actual clinical cases, the longitudinal deformation of a stent can be alleviated because of the interaction between the stent and its vessel. Stent bending is caused by vessel flexure *in vivo*, and stents interact with arteries when vessels bend. Building a model that contains plaque and vessel is useful in studying the relationship between stent flexibility and vessel injury. However, poor LS and flexibility may lead to serious vessel injury and ISR. On this basis, the model adopted in this study can still provide valuable and reliable results. Second, Kriging showed the most accurate LS approximation among the modeling methods and thus considered suitable for approximating the performance of stents with two or more deformations. However, this assumption was not intended to be an exhaustive comparison among the three modeling methods. Thus, other surrogate models for stent performance should be considered and other modeling methods should be investigated. Third, this study aims to determine the potential relationships between stent flexibility and LS and optimize the factors simultaneously. However, an ideal stent must have excellent properties, including low recoiling, foreshortening, good fatigue resistance, flexibility, LS, and hemodynamic properties. Therefore, additional objective functions will be investigated in our future work.

CONCLUSIONS

This study proposed a multi-objective optimization method based on FEA to improve stent flexibility and LS. Different surrogate models (RSM, RBF, and Kriging) were combined with DOE methods and then used for the construction of the approximate relationships between the objective functions and design variables. The accuracies of the three surrogate models were then compared. The results showed that the accuracies of the three models in fitting FM were nearly the same, but Kriging made the best prediction in LS. The relative influences of design variables on the two metrics were quantified. W_{link} played a highlighted

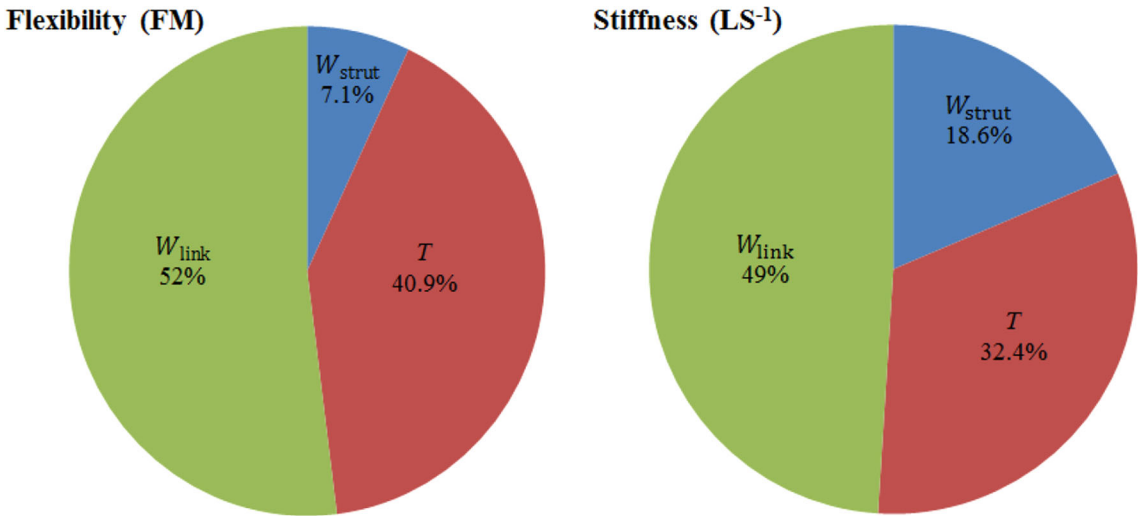

FIGURE 15. The main effects for FM and LS^{-1}.

TABLE 3. Optimization results.

Stents	W_{link} (mm)	W_{struct} (mm)	T (mm)	Kriging FM (N-rad)	FEA FM (N-rad)	Kriging LS^{-1} (mm/N)	FEA LS^{-1} (mm/N)
Original stent	0.1	0.12	0.1	0.7079	0.71	0.1544	0.1608
Optimal stent	0.1084	0.1598	0.0956	0.8016	0.7739	0.0831	0.0897

role in flexibility and LS. NSGA-II was employed to determine the trade-off between flexibility and LS. Reduction in W_{link} improves stent flexibility but reduces LS. Finally, an optimal stent was obtained by the non-dominant method and compared with the baseline geometry. The LS of the optimal stent increased by 48.3% only at the cost of 13% of FM. Conclusions made from the present work may facilitate the formulation of new stent designs, particularly those aimed at reducing longitudinal deformation. Other surrogate models and objectives, including hemodynamic performance, will be considered in our future research.

ACKNOWLEDGMENT

This project is supported by the National Natural Science Foundation of China (51305171), Natural Science Foundation of Jiangsu Province (BK20130525), Natural Science Foundation of the Higher Education Institutions of Jiangsu Province (13KJB460006), China Postdoctoral Science Foundation (2011M500858), Foundation of Jiangsu University (10JDG123) and Project of Jiangsu University for training young backbone teachers.

CONFLICT OF INTEREST

Xiang Shen, Hongfei Zhu, Jiabao Jiang, Yongquan Deng and Song Ji declare that they have no conflict of interest.

ETHICAL STANDARDS

This article does not contain any studies with human participants or animals performed by any of the authors.

REFERENCES

[1]Azaouzi, M., N. Lebaal, A. Makradi, and S. Belouettar. Optimization based simulation of self-expanding nitinol stent. *Mater. Des.* 50(17):917–928, 2013.
[2]Bressloff, N. W., G. Ragkousis, and N. Curzen. Design optimisation of coronary artery stent systems. *Ann. Biomed. Eng.* 44(2):357–367, 2016.
[3]Deb, K., A. Pratap, S. Agarwal, and T. Meyarivan. A fast and elitist multi-objective genetic algorithm: NSGA-II. *IEEE T Evol. Comput.* 6(2):182–197, 2002.
[4]Demanget, N., P. Latil, L. Orgeas, P. Badel, S. Avril, C. Geindreau, J. N. Albertini, and J. P. Favre. Severe bending of two aortic stent-grafts: an experimental and numerical mechanical analysis. *Ann. Biomed. Eng.* 40(12):2674–2686, 2012.

[5]Eshghi, N., M. H. Hojjati, M. Imani, and A. M. Goudarzi. Finite element analysis of mechanical behaviors of coronary stent. *Procedia Eng*. 10(2):3056–3061, 2011.
[6]Foin, N., C. D. Mario, D. P. Francis, and J. E. Davies. Stent flexibility versus concertina effect: mechanism of an unpleasant trade-off in stent design and its implications for stent selection in the cath-lab. *Int. J. Cardiol*. 164(3):259–261, 2013.
[7]Gundert, T. J., A. L. Marsden, W. Yang, and J. F. LaDisa. Optimization of cardiovascular stent design using computational fluid dynamics. *J. Biomech. Eng*. 134(1):031002, 2012.
[8]Hanratty, C. G., and S. J. Walsh. Longitudinal compression: a new complication with modern coronary stent platforms-time to think beyond deliverability? *Eurointervention*. 7(7):872–877, 2011.
[9]Hsiao, H. M., C. T. Yeh, C. Wang, L. Chao, and D. Li. Effects of stent design on new clinical issue of longitudinal stent compression in interventional cardiology. *Biomed. Microdevices*. 16(4):599–607, 2014.
[10]Imani, M. Simulation of mechanical behaviors of NIR stent in a stenotic artery using finite element method. *World Appl. Sci. J*. 22(7):892–897, 2013.
[11]Imani, S. M., A. M. Goudarzi, S. E. Ghasemi, A. Kalani, and J. Mahdinejad. Analysis of the stent expansion in a stenosed artery using finite element method: Application to stent versus stent study. *Proc. Inst. Mech. Eng. Part H: J Eng. Med*. 228(10):996–1004, 2014.
[12]Imani, M., A. M. Goudarzi, and M. H. Hojjati. Finite element analysis of mechanical behaviors of multi-link stent in a coronary artery with plaque. *World Appl. Sci. J*. 3(21):1597–1602, 2013.
[13]Imani, S. M., A. M. Goudarzi, P. Valipour, M. Barzegar, J. Mahdinejad, and S. E. Ghasemi. Application of finite element method to comparing the NIR stent with the multi-link stent for narrowings in coronary arteries. *Acta Mech. Solida Sin*. 28(5):605–612, 2015.
[14]Jones, D., M. Schonlau, and W. Welch. Efficient global optimization of expensive black-box functions. *J. Glob. Optim*. 13(4):455–492, 1998.
[15]Ju, F., Z. Xia, and C. Zhou. Repeated unit cell (RUC) approach for pure bending analysis of coronary stents. *Comput. Method Biomech. Biomed. Eng*. 11(4):419–431, 2008.
[16]Kwok, O. H. Stent concertina: stent design does matter. *J. Invasive Cardiol*. 25(6):114–119, 2013.
[17]Maleckis, K., P. Deegan, W. Poulson, C. Sievers, A. Desyatova, J. MacTaggart, and A. Kamenskiy. Comparison of femoroapopliteal artery stents under axial and radial compression, axial tension, bending, and torsion deformations. *J. Mech. Behav. Biomed*. 75:160–168, 2017.
[18]Matheron, G. Principles of geostatistics. *Econ. Geol*. 58(8):1246–1266, 1963.
[19]Morris, M. D., and T. J. Mitchell. Exploratory designs for computational experiments. *J. Stat. Plan Inference* 43(3):381–402, 1995.
[20]Murphy, E. A., and F. J. Boyle. Reducing in-stent restenosis through novel stent flow field augmentation. *Cardiovasc. Eng. Technol*. 3(4):353–373, 2012.
[21]Myers, R. H., and D. C. Montgomery. Response surface methodology: process and product optimization using designed experiment. *J. Stat. Plan Inference* 59:185–186, 1995.
[22]Ni, Z., X. Gu, and Y. Wang. Rapid prediction method for nonlinear expansion process of medical vascular stent. *Sci China Ser E: Technol Sci*. 52(5):1323–1330, 2009.
[23]Ni, X., C. Pan, and P. B. Gangadhara. Numerical investigations of the mechanical properties of a braided non-vascular stent design using finite element method. *Comput. Methods Biomech. Biomed. Eng*. 18(10):1117–1125, 2015.
[24]Ni, X., G. Wang, Z. Long, and C. Pan. Analysis of mechanical performance of braided esophageal stent structure and its wires. *J. Southeast Univ. (English Ed)* 28(4):457–463, 2012.
[25]Ni, X., Y. Zhang, H. Zhao, and C. Pan. Numerical research on the biomechanical behaviour of braided stents with different end shapes and stent-oesophagus interaction. *Int. J. Numer. Method Biomed. Eng*. 34(6):e2971, 2018.
[26]Ormiston, J. A., B. Webber, and M. W. Webster. Stent longitudinal integrity: bench insights into a clinical problem. *Jacc-Cardiovasc Int*. 4(12):1310–1317, 2011.
[27]Pant, S., N. W. Bressloff, and G. Limbert. Geometry parameterization and multidisciplinary constrained optimisation of coronary stents. *Biomech. Model. Mechanobiol*. 11(1–2):61–82, 2012.
[28]Pant, S., G. Limbert, N. Curzen, and N. W. Bressloff. Multi-objective design optimization of coronary stents. *Biomaterials*. 32(31):7755–7773, 2011.
[29]Park, J. K., K. S. Lim, I. H. Bae, J. P. Nam, J. H. Cho, C. Choi, J. W. Nah, and M. H. Jeong. Stent linker effect in a porcine coronary restenosis model. *J. Mech. Behav. Biomed*. 53:68–77, 2016.
[30]Petrini, L., F. Migliavacca, F. Auricchio, and G. Dubini. Numerical investigation of the intravascular coronary stent flexibility. *J. Biomech*. 37(4):495–501, 2004.
[31]Ragkousis, G. E., N. Curzen, and N. W. Bressloff. Multi-objective optimisation of stent dilation strategy in a patient-specific coronary artery via computational and surrogate modeling. *J. Biomech*. 49(2):205–215, 2016.
[32]Rigattieri, S., A. Sciahbasi, and P. Loschiavo. The clinical spectrum of longitudinal deformation of coronary stents: from a mere angiographic finding to a severe complication. *J. Invasive Cardiol*. 25(5):101–105, 2013.
[33]Shen, X., Y. Deng, Z. Xie, S. Ji, and H. Zhu. Flexibility behavior of coronary artery stents: the role of linker investigated with numerical simulation. *J. Mech. Med. Biol*. 17(08):1750112, 2017.
[34]Shen, X., Z. Xie, Y. Deng, and S. Ji. Effects of metal material stent design parameters on longitudinal stent strength. *Key Eng. Mater*. 723:299–304, 2017.
[35]Shen, X., H. Yi, and Z. Ni. Multi-objective design optimization of coronary stent mechanical properties. *Chin. J. Dial Artif. Organs*. 4(3):835–838, 2012.
[36]Simpson, T. W., D. K. J. Lin, and W. Chen. Sampling strategies for computer experiments: design and analysis. *Int. J. Reliab. Appl*. 2(3):209–240, 2001.
[37]Williams, P. D., M. A. Mamas, K. P. Morgan, M. El-Omar, B. Clarke, A. Bainbridge, F. Fath-Ordoubadi, and D. G. Fraser. Longitudinal stent deformation: a retrospective analysis of frequency and mechanisms. *Eurointervention* 8(2):267–274, 2012.
[38]Wu, W., D. Yang, M. Qi, and W. Wang. An FEA method to study flexibility of expanded coronary stents. *J. Mater. Process Technol*. 184:447–450, 2007.
[39]Zhao, S., L. Gu, and S. R. Foremming. Effects of arterial strain and stress in the prediction of restenosis risk: computer modeling of stent trials. *Biomed. Eng. Lett*. 2(3):158–163, 2012.